fibers

MDPI

Article

Experimental and Statistical Investigations for Tensile Properties of Hemp Fibers

Peyman Sadeghi, Quang Cao, Ragab Abouzeid, Mohammad Shayan, Meensung Koo and Qinglin Wu *

School of Renewable Natural Resources, Louisiana State University AgCenter, Baton Rouge, LA 70803, USA; psadeg1@lsu.edu (P.S.); qcao@lsu.edu (Q.C.); rabouzeid@agcenter.lsu.edu (R.A.); mshaya1@lsu.edu (M.S.); mkoo1@lsu.edu (M.K.)

* Correspondence: wuqing@lsu.edu

Abstract: This study investigated the tensile behaviors of hemp fiber bundles and examined how properties including tensile strength and Young's modulus vary with the bundle diameter. Hemp fibers were extracted, degummed, and separated into bundles of different diameters ranging from less than 50 µm to over 150 µm. Tensile tests were conducted on these fiber bundles using a rheometer-based tensile testing machine. The results showed that hemp fibers exhibited a tensile strength of 97.33 MPa and a Young's modulus of 3.77 GPa at a 50% survival probability. However, the scale parameters for breaking stress and Young's modulus were determined to be 620.57 MPa and 29.88 GPa, respectively. As the fiber bundle diameter increased, the tensile strength decreased significantly. This was attributed to the higher probability of defects and irregularities acting as weakness points in larger fiber bundles. In contrast, Young's modulus (stiffness) increased with increasing bundle diameter, likely due to improved fiber–fiber interactions. To further understand the variability and reliability of the tensile properties, statistical models were developed. The Weibull distribution analysis was applied, revealing critical insights into the variability of diameter, stress at break, Young's modulus, and strain at break. The Weibull parameters provided a comprehensive understanding of the fibers' mechanical reliability. Additionally, the Griffith model was employed to predict the strength and Young's modulus based on fiber diameters, supporting the observation that thinner fibers generally exhibited higher tensile strength due to fewer defects. Overall, this work highlights the importance of understanding structure–property relationships in natural fibers like hemp for optimizing their performance in composites.

Keywords: hemp fiber; fiber bundles; Weibull model; Griffith model

Citation: Sadeghi, P.; Cao, Q.; Abouzeid, R.; Shayan, M.; Koo, M.; Wu, Q. Experimental and Statistical Investigations for Tensile Properties of Hemp Fibers. *Fibers* **2024**, *12*, 94. https://doi.org/10.3390/fib12110094

Academic Editor: Sushanta Ghoshal

Received: 16 August 2024
Revised: 13 October 2024
Accepted: 25 October 2024
Published: 1 November 2024

1. Introduction

In recent years, there has been a notable shift towards the utilization of natural fibers as sustainable and eco-friendly alternatives to synthetic fibers in both fiber-reinforced composites and functional textiles [1,2]. Among these natural fibers, hemp fibers, derived from the stem of the *Cannabis sativa* plant, have emerged as particularly promising bast fibers due to their superior mechanical properties and environmental benefits [3].

Natural fibers, such as hemp fibers, are gaining prominence in high-performance composite materials for various applications [4]. These fibers are particularly promising due to their biodegradability, renewability, abundance, and low cost, promoting a circular, low-carbon economy [5,6]. Among these, bast fibers like flax, hemp, jute, and ramie, and leaf fibers such as abaca, sisal, banana, and pineapple, are widely used in cementitious and polymer-based composites owing to their high cellulose content, which enhances tensile strength [7]. Additionally, natural fibers have a complex microstructure comprising multiple lumens and cell layers with specific micro-fibril orientations [8]. Their properties are significantly influenced by growth conditions including soil quality, rainfall, sunlight, temperature, and humidity, as well as by harvesting time, extraction methods, and subsequent treatments [9,10]. This variability can lead to inconsistencies in the mechanical,

thermal, and fatigue properties of the fibers, making the reliable comparison of test results challenging. Hence, statistical analysis is vital for providing dependable data and understanding the mechanical properties of natural fibers [11–13].

Hemp fibers consist of a series of concentric layers with a central cavity known as the lumen. The outermost layer, the primary cell wall, is quite thin, measuring only 0.1 to 0.2 µm in thickness [14]. Beneath this, the secondary cell wall is composed of three sublayers (S1–S3), with the S2 layer forming about 80% of the structure. This main layer contains highly crystalline cellulose fibrils, which are arranged in a spiral pattern within a matrix of amorphous hemicelluloses and pectin. These fibrils are oriented at an angle of approximately 10–11° relative to the fiber axis, an arrangement referred to as the microfibrillar angle [15]. Hemp cellulose is known for its high crystallinity, falling between the more crystalline flax cellulose [16] and the semi-crystalline cellulose of kenaf. Numerous studies utilizing X-ray diffraction have reported hemp fiber crystallinity ranging from 56% to 80% [17].

Hemp fibers are among the strongest natural fibers, noted for their excellent mechanical properties, good insulation capabilities, low density, ease of production, and high market availability [18]. Originally native to Asia, hemp is now extensively cultivated in various regions, including China, Europe, the United States, and Canada. This annual crop can be harvested within two to three months of seeding. The fibers are extracted from the hemp stem through a microbial process known as retting, followed by mechanical or manual separation. Numerous studies have demonstrated the effectiveness of hemp-fiber-reinforced composites in reinforcing masonry panels, arches, and other structural elements [19].

Statistical approaches, including the Weibull and Griffith distribution [20,21] are frequently used to model the tensile properties of natural fibers. These methods effectively account for the size effects, heterogeneities, and brittle failure characteristics of the materials. Conversely, while the Gaussian distribution is utilized in some studies and recommended by certain standards, it is less appropriate due to its allowance for negative values, which are not physically consistent with the properties of natural fibers [22].

A comprehensive understanding of biocomposite materials necessitates detailed knowledge of both the reinforcing fibers and the matrix [23,24]. Extensive research has evaluated the mechanical properties of hemp fibers [25–30] addressing the inherent variability due to growth conditions, processing procedures, and retting. However, there has been limited focus on comprehensively assessing the uncertainties related to the tensile strength and elastic modulus of various hemp fiber structures. This understanding is crucial for accurately describing the mechanical properties of composite structures that utilize these inherently variable fibers.

To measure the tensile properties of short and brittle mineral fibers, [31] employed the Sentmanat Extensional Rheometer (SER-tool), adapting it slightly to facilitate the mounting of short fibers on paper supports. Their parametric error analysis revealed that the primary source of error stemmed from inaccuracies in measuring fiber diameter, underscoring the critical need for precision in this metric [32] introduced an innovative method leveraging acoustic emission signals during bundle testing to quickly characterize the strength and elongation distributions of single fibers within a bundle. This approach integrates acoustic emission technology with fiber bundle theory modeling, demonstrating a strong correlation between cumulative breaking strength distributions from bundle and single fiber tests, though the elongation distribution from bundle tests appeared broader.

Hemp fiber characterization presents unique challenges in single fiber tensile testing, primarily due to their inherent variability and irregular morphology. Unlike their synthetic counterparts, these fibers exhibit non-uniform cross-sections and dimensions along their length, compounded by the presence of inherent flaws [33]. This variability necessitates precise measurement techniques for accurate property determination. While various microscopy methods have been employed to assess fiber dimensions, the common assumption of circular cross-sections may lead to inaccurate property calculations. Further-

more, the testing process itself requires careful consideration, from specimen mounting to force measurement and elongation detection. Researchers have developed innovative approaches to address these challenges, including specialized mounting techniques and non-contact measurement systems. These methodologies aim to minimize experimental errors and enhance the reliability of natural fiber characterization, ultimately contributing to a more comprehensive understanding of their mechanical properties [34,35].

This study aims to investigate the mechanical properties of hemp fibers using a rheometer, with a focus on tensile strength, elongation, and Young's modulus, and their dependency on fiber diameter. We examine the primary factors influencing these properties and apply Weibull and Griffith models to predict tensile strength and Young's modulus based on fiber diameter. Our findings indicate that thinner fibers generally exhibit higher tensile strength due to fewer defects, and the statistical analysis confirms a strong correlation between predicted and experimental data, validating the effectiveness of these models. While previous studies have demonstrated the influence of diameter on hemp fiber mechanics, this work introduces significant advancements by utilizing a rheometer for tensile testing, which enhances accuracy and reduces error, following ASTM D 3379-75 standards [36]. Testing nearly 200 fiber bundles provides a statistically robust dataset, enabling a more reliable analysis of diameter-dependent mechanical behaviors. The combined use of Weibull and Griffith models offers a unique, in-depth understanding of how fiber diameter affects tensile strength and Young's modulus, providing quantitative insights that surpass prior research. These advancements, along with the large-scale testing and refined statistical approach, contribute to novel findings with practical implications for optimizing natural fiber composites, distinguishing this work from earlier studies.

2. Experimental

2.1. Materials

Raw hemp bast fibers, mechanically separated from the hemp stalk, were purchased in large quantities from a commercial supplier. These fibers had some hurd material dispersed randomly within them. The hurd material was removed through combing the fibers. Sodium hydroxide and sodium sulfide were purchased from VWR Life Science (Solon, OH, USA). Hydrogen peroxide (30% aqueous solution) was obtained from J.T. Baker (Radnor, PA, USA).

2.2. Preparation of Degumming Hemp Fibers

The combed hemp fibers without hurd were pretreated using a 12% sodium hydroxide with a liquid ratio of 1:8 (v/w) at 90 °C for 2 h. Subsequently, the fibers underwent bleaching using a mixture of 2% NaOH and 10% H_2O_2 at a temperature of 90 °C for 1 h. Finally, the bleached fibers or degummed hemp fibers were thoroughly rinsed with tap water until reaching a neutral pH and dried in an oven at 60 °C. The degummed hemp fibers were carded by using a MESDAN machine equipped with a comb drum to separate fiber bundles into individual fibers, as is shown in Figure 1.

2.3. Sample Preparation for Tensile Test

Hemp fiber specimens for tensile tests were prepared using a paper frame technique, where thick paper was used, and fiber specimens were attached with glue. Multiple specimens were prepared for each sample, with a gauge length of L_0 = 25 mm (Figure 1). The diameter of the hemp fibers, fiber geometry, and surface morphology were investigated using an electron microscope (model: JSM-6610 LV SEM JEOL, Tokyo, Japan) under high vacuum conditions at an accelerated voltage of 5 kV.

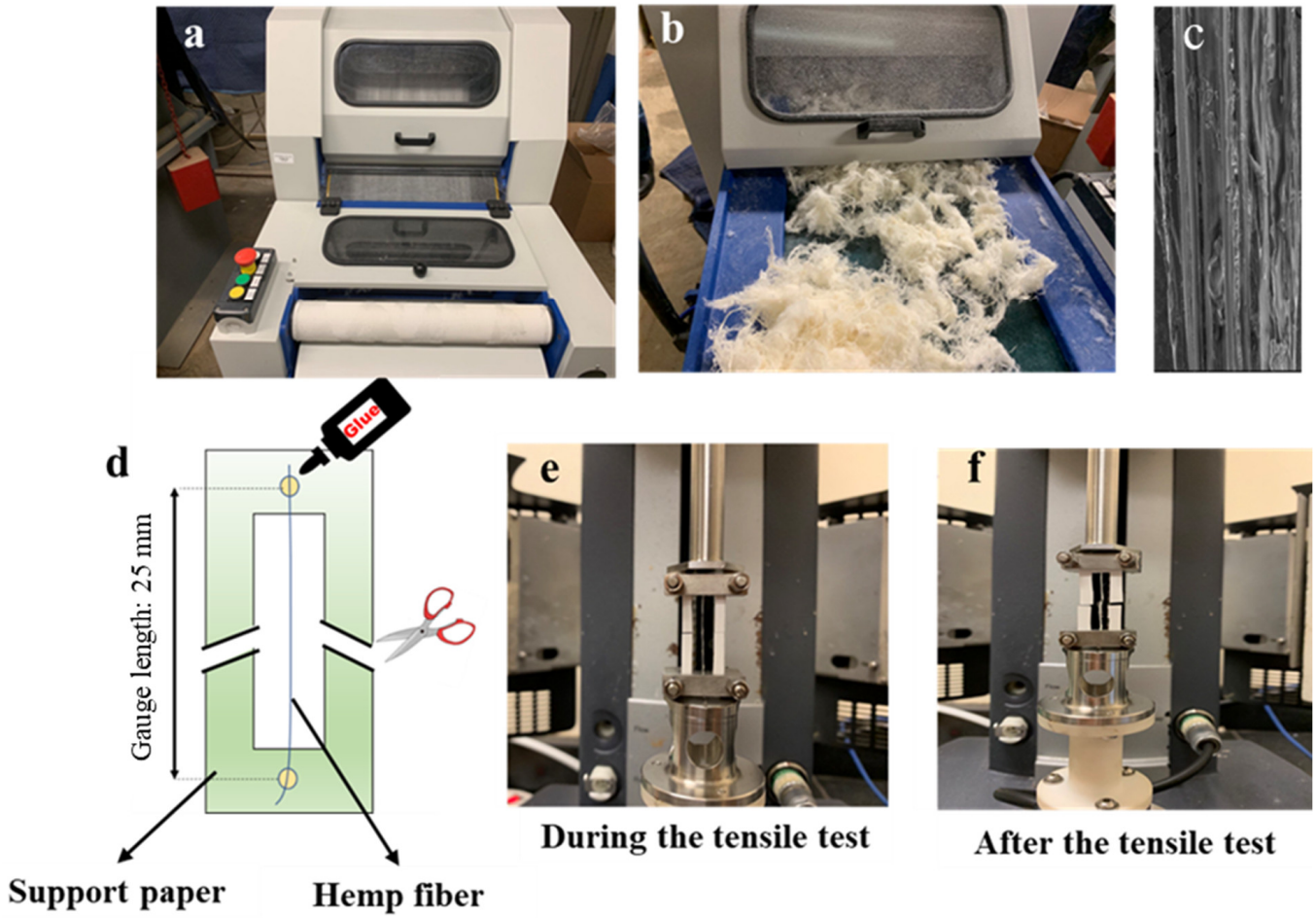

Figure 1. Hemp fiber preparation and testing. (**a**) Carding machine, (**b**) carded fibers, (**c**) optical micrograph of hemp fiber at 100 magnification, (**d**) fiber tensile testing schematic, (**e**,**f**) tensile method before and after testing with the rheometer.

2.4. Tensile Behavior of Hemp Fibers

The tensile properties of the fibers were measured using a model AR2000EX rheometer (TA Instruments-Waters LLC, New Castle, DE, USA) with tensile fixtures, following the ASTM D 3379-75 standard [36]. The gauge length, or the distance between the two grips, was set at 25 mm. Key parameters, such as tensile strength and elongation at break, were calculated using the force and displacement data recorded by the machine. These calculations were based on the initial cross-sectional area and the original gauge length of each sample. The tensile speed was maintained at 0.1 mm/min, and more than two hundred samples were tested. Fibers broken close to or at gripping regions were excluded, and only data from successful tests were recorded. In Figure 2a, a detailed schematic configuration illustrates the arrangement of individual fibers within the test piece, highlighting the structural alignment and orientation of single fibers essential to the overall mechanical properties and performance evaluation in the experimental setup. An optical microscope (model: Leica DM6, Leica Teaneck, NJ, USA) was employed to measure the diameter of each tested hemp fiber within the gauge length area, as shown in Figure 2b. The cross-sectional area of the fiber was estimated under the assumption of a circular shape. For each obtained image, 10 positions were randomly selected and the average of diameters was reported as the fiber diameter.

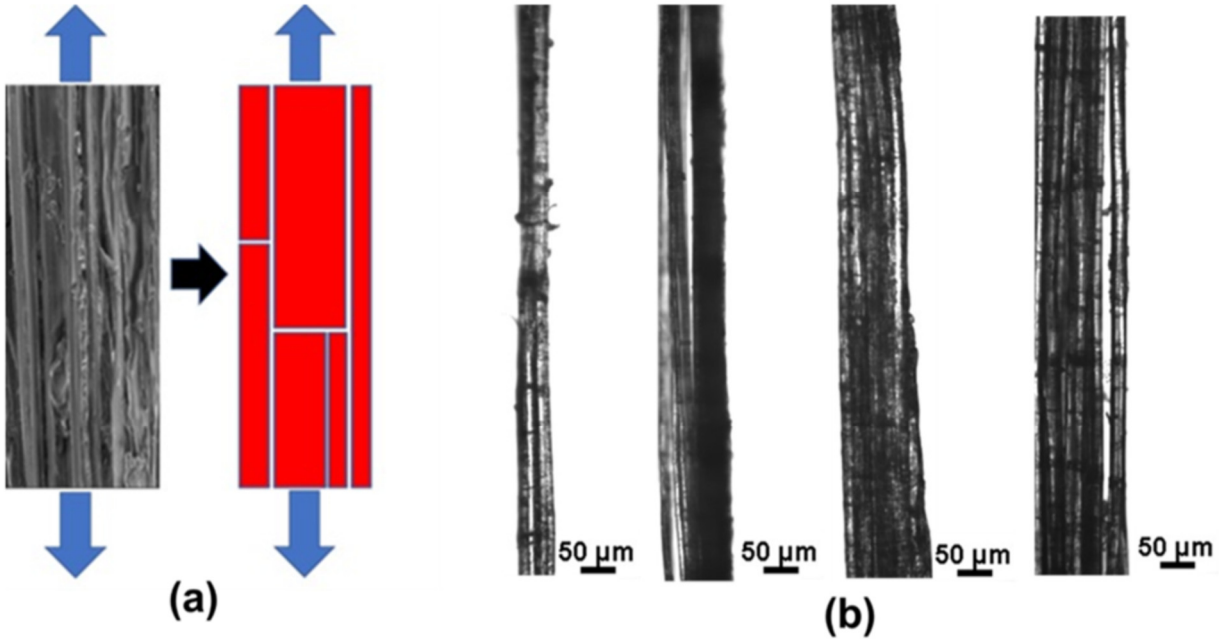

Figure 2. (**a**) Schematic configurations of single fibers in a test piece, (**b**) optical microscopy images of hemp fiber bundles.

3. Statistical Analysis

3.1. The Weibull Model

The Weibull distribution is a widely used statistical approach for characterizing the variability in mechanical properties of brittle materials like hemp fibers [37]. This model helps in understanding the variability and reliability of tensile strength data by fitting a statistical distribution to the observed strengths of fibers. The Weibull distribution is characterized by its shape parameter and scale parameter, which describe the form distribution and scale, respectively. For hemp fibers, the Weibull model can effectively capture the probability of failure at different stress levels, considering the presence of defects and irregularities within the fibers [38]. This method is based on the premise that failure initiates from the most critical flaw present in the material, leading to complete failure [39]. Hemp fibers exhibit significant variations in properties such as diameter, tensile strength, Young's modulus, and strain, due to the inherent presence of defects throughout their structure, which is a common issue with natural fibers [40]. Consequently, the mechanical testing data have been statistically analyzed using the conventional Weibull distribution. This approach is used to characterize the distribution of fiber properties (x). The expression for this analysis is as follows:

$$F(x) = 1 - exp\left[-\left(\frac{V}{V0}\right)\left(\frac{x}{x0}\right)^{m}\right] \quad (1)$$

Assuming a constant fiber volume,

$$F(x) = 1 - exp\left[-\left(\frac{x}{x0}\right)^{m}\right] = 1 - P(x) \quad (2)$$

In this equation, $F(x)$ or the CDF of x represents the probability of failure, and $P(x)$ represents the probability of survival with respect to x, adhering to the total probability principle: $P(x) + F(x) = 1$. The shape parameter, known as the Weibull modulus, m, is dimensionless and reflects the data's dispersion. The smaller the value of m, the wider distribution of x, whereas a larger m suggests a narrower distribution. The scale parameter $x0$ signifies the characteristic values predicted by the Weibull model for the parameter x, relative to a reference gauge volume, $V0$, with V being the fiber volume. The parameter x

can encompass various characteristics such as diameter, tensile strength, Young's modulus, and strain of the fibers.

Hence, the Probability Density Function (PDF) for the random variable x following a two-parameter Weibull distribution is as follows:

$$F(X) = \left(\frac{m}{x_0}\right)\left(\frac{x}{x_0}\right)^{m-1} exp\left[-\left(\frac{x}{x_0}\right)^{m}\right], x, x_0, m > 0, \quad (3)$$

3.2. The Griffith Model

Natural fibers, such as hemp, exhibit a high degree of variability in their mechanical properties due to the inherent heterogeneity in their structure. Researchers have observed a significant dependency of these properties on the fiber diameter. Several scholars have attempted to apply the Griffith model to describe the variations in tensile strength (σf) and Young's modulus (E) with respect to the fiber diameter (df) [41]. The relationships proposed by the Griffith model are given as follows:

$$\sigma f(df) = A + \frac{B}{df} \quad (4)$$

$$E(df) = A + \frac{B}{df} \quad (5)$$

In these equations, A and B are the Griffith parameters obtained through curve fitting, and df represents the fiber diameter. The tensile strength (σf) and Young's modulus (E) are expressed as functions of the fiber diameter to capture the size-dependent behavior observed in natural fibers like hemp.

4. Results and Discussions

4.1. Surface Analysis

Examination of the hemp fibers under a scanning electron microscope (SEM), as depicted in Figure 3, provided additional evidence for the presence of fiber bundles in many of the tensile test samples. This analysis provides visual evidence that many tensile specimens contain fiber bundles, rather than single fibers. This heterogeneous sampling likely contributed to the wide variation in the measured tensile strengths. Isolation and testing of single fibers is ideal, but the process is very hard due to the nature of the hemp fibers. SEM imaging revealed that the typical diameters of individual hemp fibers fell in a relatively narrow range, consistent with fiber dimensions reported in the literature. However, the diameters of the tensile test specimens were often significantly larger. This indicates that the tested segments likely contained multiple fibers bonded together, rather than isolating single fibers. Some images clearly showed fiber bundles made up of two or more individual fibers.

Surface analysis of the hemp fiber bundles by SEM images reveals the intricate structure of the fibers and their bundling. The images highlight that many of the tensile specimens consist of multiple fibers bonded together by natural matrices, such as lignin and pectin, as observed in other plant fibers. This bundling effect contributes to uneven stress distribution during tensile testing, leading to variability in the mechanical properties measured. Furthermore, the SEM images clearly show the presence of voids between the fibers, which can weaken the composite fiber structure. The diameter variations observed in the hemp fiber bundles, as well as in individual fibers, also suggest a heterogeneous sample population, which complicates the direct comparison to single-fiber tensile behavior.

The bundling of fibers occurs naturally in hemp and in many plant bast fibers. Fiber bundles have more defects at the interfaces and fiber interactions, which create stress concentrations. This helps explain the lower tensile strength of the fiber bundles compared to that of the single fibers.

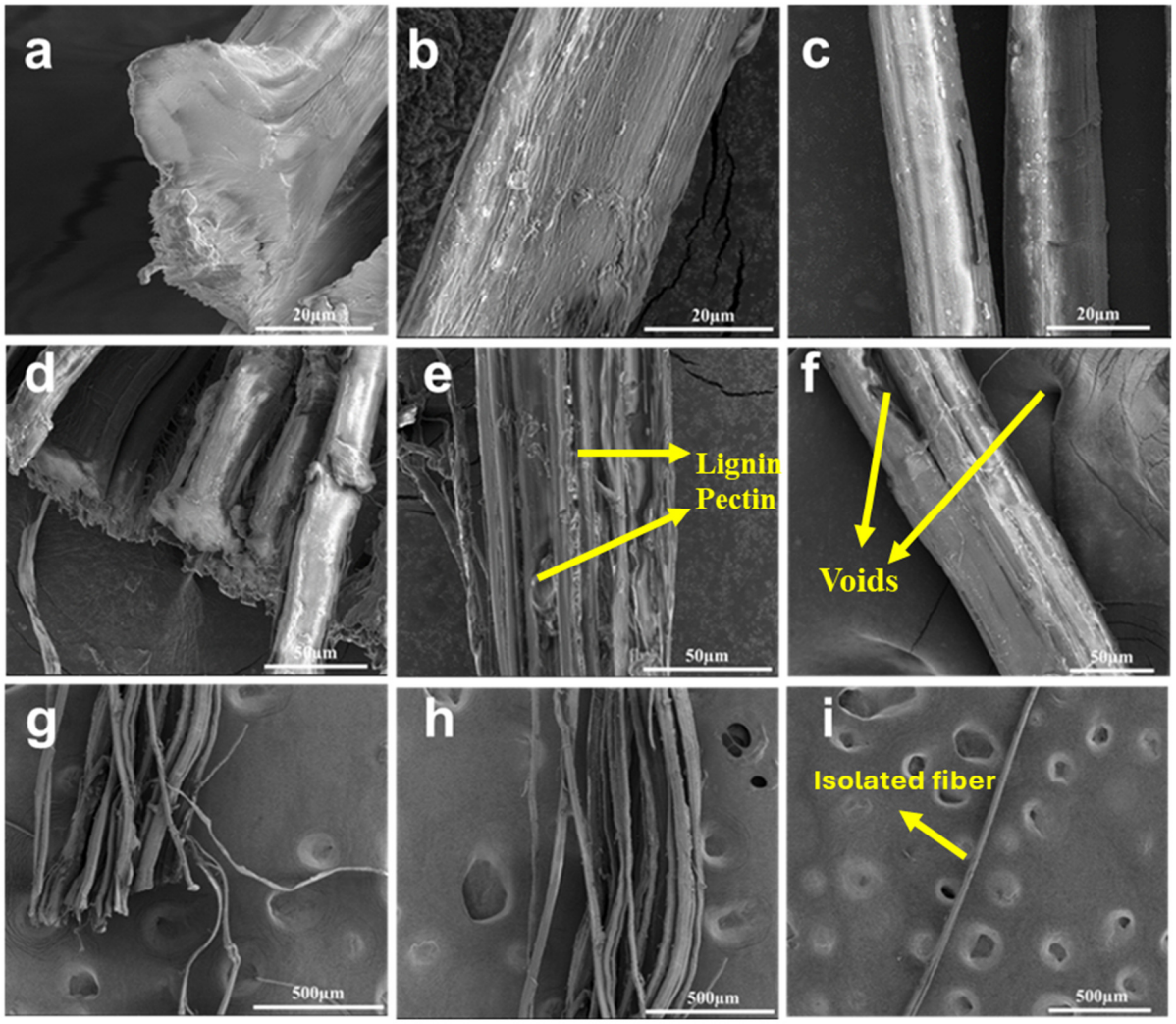

Figure 3. SEM images of hemp bundles. (**a**,**d**) Cross sectional images of hemp fibers, (**b**,**c**) surface of hemp single fiber, (**e**,**f**) voids and defects in hemp bundles, (**g**,**h**) hemp bundles, and (**i**) hemp single fiber.

Proper isolation of individual fibers is challenging with interconnected bast fiber networks like hemp. Some degree of bundled fibers is to be expected. This further underscores the need for statistical approaches in tensile testing, as fiber bundles decrease the average strength compared to flawless single fibers.

4.2. Tensile Strength of Hemp Fiber Bundles

The stress–strain graphs reveal distinct differences in the mechanical behaviors of hemp fibers as the bundle diameter increases. For the smallest diameter range, below 50 µm, as shown in Figure 4a, the stress–strain curves exhibit a highly linear elastic region until the yield point, indicating exceptional structural integrity and minimal defects within these fine fiber bundles. The slope of the linear elastic region corresponds to the tensile modulus or stiffness of the fibers, which is observed to be highest in this diameter range. Beyond the yield point, these small fiber bundles undergo a pronounced strain-hardening phase, where the stress continues to increase gradually with increasing strain. This behavior is attributed to the progressive alignment and reorientation of the cellulose fibrils along the loading direction, enabling the fibers to accommodate further deformation before failure. Notably, the stress at break for these bundles is the highest among all diameter ranges, typically ranging from 1100 to 1800 MPa. This exceptional tensile strength is the result of

the high degree of structural perfection, minimal defects, and efficient stress transfer within these fine fiber bundles.

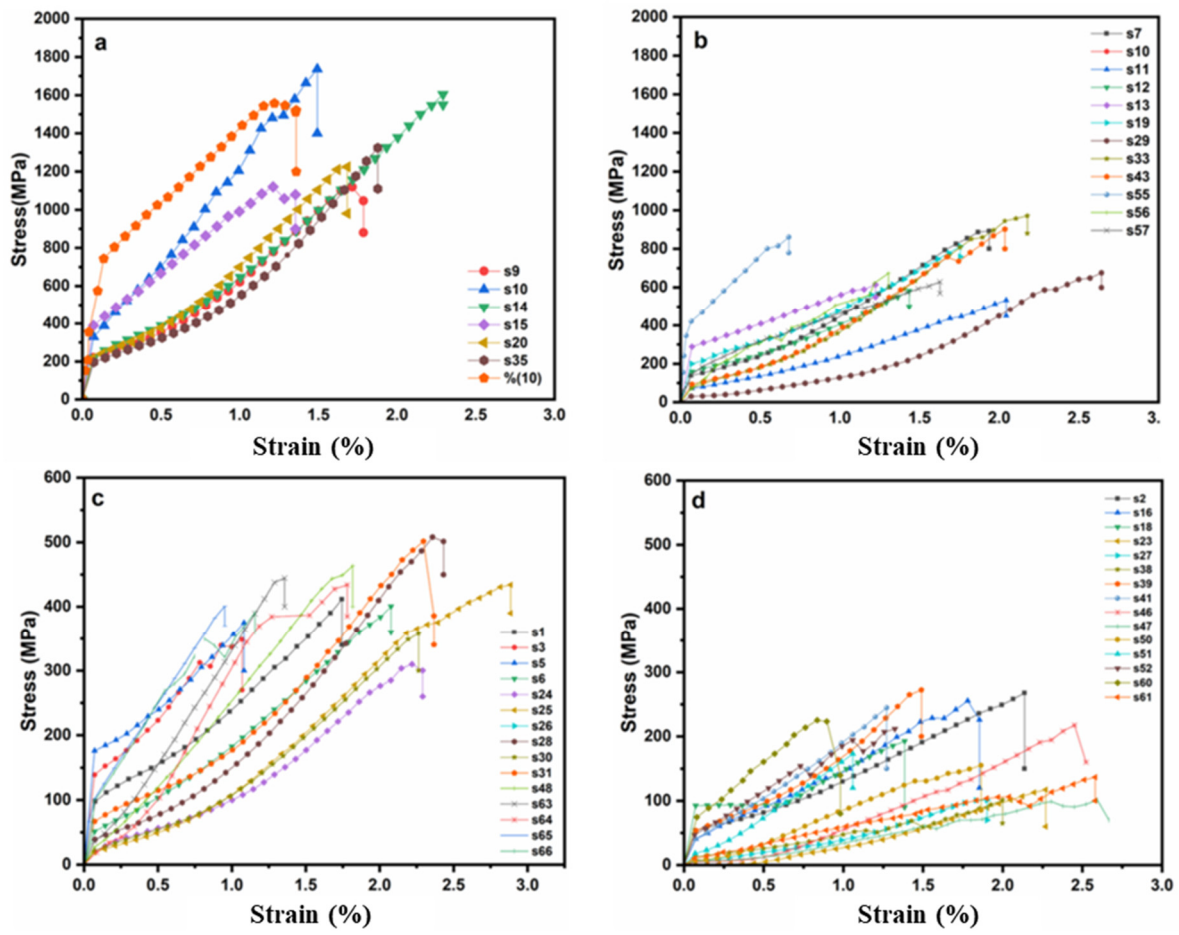

Figure 4. Stress–strain graphs for hemp fibers in different diameter range groups. (**a**) D < 50 µm, (**b**) 50 µm < D < 100 µm, (**c**) 100 µm < D < 150 µm, (**d**) D > 150 µm.

In the 50–100 micrometer range shown in Figure 4b, the stress–strain curves begin to exhibit a slight nonlinearity in the elastic region, indicative of the presence of some structural defects or irregularities within the bundles. The yield point becomes more pronounced, suggesting a more sudden transition from elastic to plastic deformation. Despite the presence of defects, these fiber bundles still exhibit a strain-hardening phase with a lower slope compared to the smaller diameter fibers. The stress at break for this diameter range is typically in the range of 400–1000 MPa, lower than the first group bundles but still demonstrating considerable tensile strength.

As the bundle diameter increases to the 100–150 micrometer range (Figure 4c), the nonlinearity in the elastic region becomes even more prominent, reflecting a higher density of defects and structural irregularities within the larger bundles. The yield point is distinct, but the subsequent strain-hardening region is less pronounced, suggesting a reduced ability for fibril reorientation and deformation accommodation. The stress at break for these 100–150 micrometer bundles falls within the range of 300–500 MPa, further decreasing compared to the smaller diameter ranges.

The broader range in failure strains observed in this diameter range also indicates variability in defect distributions among individual bundles.

For bundle diameters exceeding 150 µm, shown in Figure 4d, the stress–strain behavior becomes highly nonlinear and irregular, indicative of a significant density of defects and structural imperfections. The yield point is less well-defined, and the strain-hardening region is gradual and limited, suggesting that the fibers have a reduced capacity for

deformation accommodation through fibril reorientation. The stress at break for these largest bundles is the lowest among all diameter ranges, typically ranging from 200 to 400 MPa. The significant variability in failure strains, ranging from around 1% to 5%, also reflects the variable defect distributions within these largest fiber bundles.

The decrease in stress at break with increasing bundle diameter can be attributed to the higher probability of encountering defects, such as kink bands, dislocations, misaligned fibrils, or weak interfacial regions between individual fibers within the bundle. These defects act as stress concentrators and initiation sites for failure, leading to premature fracture at lower stress levels. Additionally, larger bundles may experience inefficient stress transfer between individual fibers, as well as potential shear deformation and fiber–fiber interactions that can further contribute to the observed nonlinear behavior and reduced tensile strength.

4.3. Prediction of Tensile Strength Based on Stress at Break–Diameter Graph

The relationship between the tensile strength (stress at break) and fiber diameter for hemp fiber bundles, plotted in Figure 5, exhibits a strong inverse power-law behavior. As the bundle diameter increases, the tensile strength decreases in a nonlinear fashion, following a negative power trend. This observation aligns with the earlier discussion on the increasing presence of defects and structural irregularities in larger fiber bundles, which act as stress concentrators and initiation sites for premature failure. To quantify this relationship, various regression models, including linear, polynomial, power, exponential, and logarithmic models were fitted. Among these, the power regression model [42] yielded the highest coefficient of determination (R-squared value of 0.717), indicating that it provides the best fit to the experimental data.

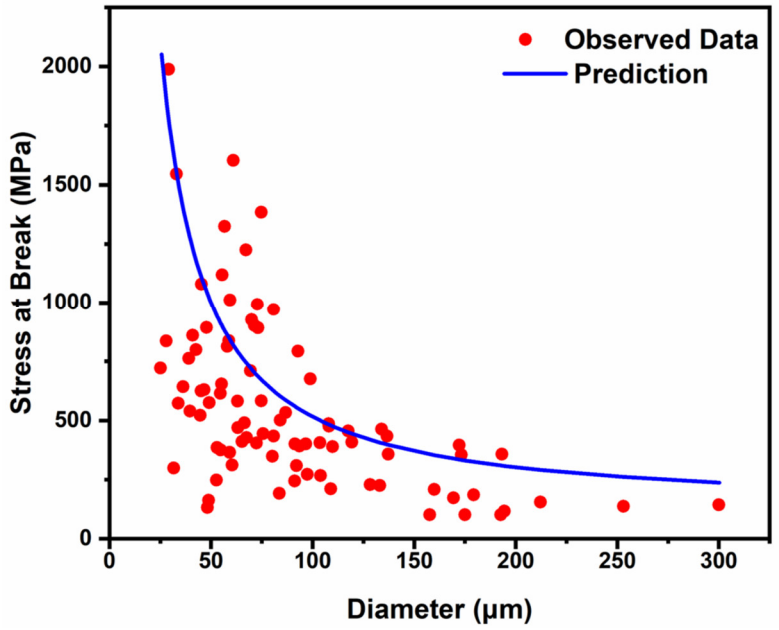

Figure 5. Tensile strength of hemp bundles as a function of their diameter.

The power regression equation is as follows:

$$TS = 6642.7\ D^{-1.168} \quad (6)$$

This equation captures the inverse relationship between tensile strength and fiber bundle diameter. The negative exponent (−1.168) in the power equation reflects the decreasing trend in tensile strength as the diameter increases.

An R-squared value of 0.717 suggests that approximately 71.7% of the variability in the tensile strength data can be explained by the power regression model based on the

fiber bundle diameter. This relatively high R-squared value indicates a strong correlation between the two variables and supports the validity of the power regression model in predicting the tensile strength from the fiber bundle diameter. However, it is important to note that the remaining 28.3% of the variability in the data is not accounted for by the model, which could be attributed to other factors influencing the tensile strength, such as variations in fiber quality, processing conditions, or inherent defects within individual bundles. The power regression model provides a quantitative tool for predicting the tensile strength of hemp fiber bundles based on their diameter. This predictive capability can be valuable in material selection and design applications, enabling engineers and researchers to estimate the mechanical performance of hemp fibers based on their bundle size. To assess the predictive accuracy of the power regression model, the Root Mean Square Error (RMSE), as a standard way to measure the error of a model in predicting quantitative data, was calculated [43]. The RMSE was found to be 356.6371 MPa, indicating the average deviation between predicted and observed tensile strength values. This error, representing approximately 18.8% of the observed tensile strength range (100–2000 MPa), suggests a moderate level of prediction accuracy. The relatively high RMSE reflects the considerable variability inherent in natural hemp fibers, particularly evident for smaller diameter fibers. While the model captures the general inverse relationship between fiber diameter and tensile strength, the RMSE underscores the complexity of predicting mechanical properties in heterogeneous biological materials like hemp fibers.

4.4. Weibull Distribution Analysis

The Weibull distribution analysis is a powerful statistical tool that provides insights into the variability and reliability of material properties. In this study, we applied the two-parameter Weibull distribution to the tensile properties of hemp fibers, specifically focusing on diameter, stress at break, Young's modulus, and strain at break. The shape (β) and scale (η) parameters obtained from this analysis are summarized in Table 1.

Table 1. Weibull parameters of hemp fiber properties.

Property	Weibull Shape (β)	Weibull Scale (η)
Diameter	2.14129	101.20105
Stress at Break	1.74620	620.57366
Young's Modulus	2.62964	29.87748
Strain at Break	3.21909	1.89552

For the diameter of hemp fibers, the shape parameter (β) is 2.14 and the scale parameter (η) is 101.20 µm. A shape parameter less than one means that the distribution resembles a negative exponential distribution, while a shape parameter greater than or equal to one does not necessarily mean a relatively narrow distribution. This consistency is crucial for composite applications where uniformity in fiber dimensions can significantly affect the mechanical properties of the composite material.

The variability in the breaking stress of hemp fibers is illustrated in Figure 6, which shows a broader distribution for stress at break compared to diameter. This broader distribution is indicative of inherent flaws and defects commonly found in natural fibers. The stress at break has a shape parameter of 1.75 and a scale parameter of 620.57 MPa. The lower shape parameter signifies a wide range of breaking stresses, emphasizing the natural variability in hemp fibers. The scale parameter, representing the characteristic strength at which 63.2% of the fibers would fail, highlights the overall robustness of hemp fibers under tensile loads. For the Young's modulus, the shape parameter is 2.63 and the scale parameter is 29.88 GPa. A narrower distribution for Young's modulus can be seen, indicating less variability in the stiffness of the hemp fibers compared to their breaking stress. This high shape parameter suggests that the Young's modulus is relatively consistent, which is advantageous for applications requiring predictable and stable material behavior under mechanical loading. The consistent stiffness of hemp fibers makes them suitable for

applications where uniform mechanical properties are crucial. The results of the Weibull analysis highlight the critical aspects of hemp fiber properties. The high shape parameters for Young's modulus and strain at break suggest that these properties are less susceptible to variability, providing reliable performance in applications. In contrast, the relatively lower shape parameter for stress at break indicates that there are more variations in the tensile strength, which could be mitigated by refining the processing techniques to reduce defects in the fibers.

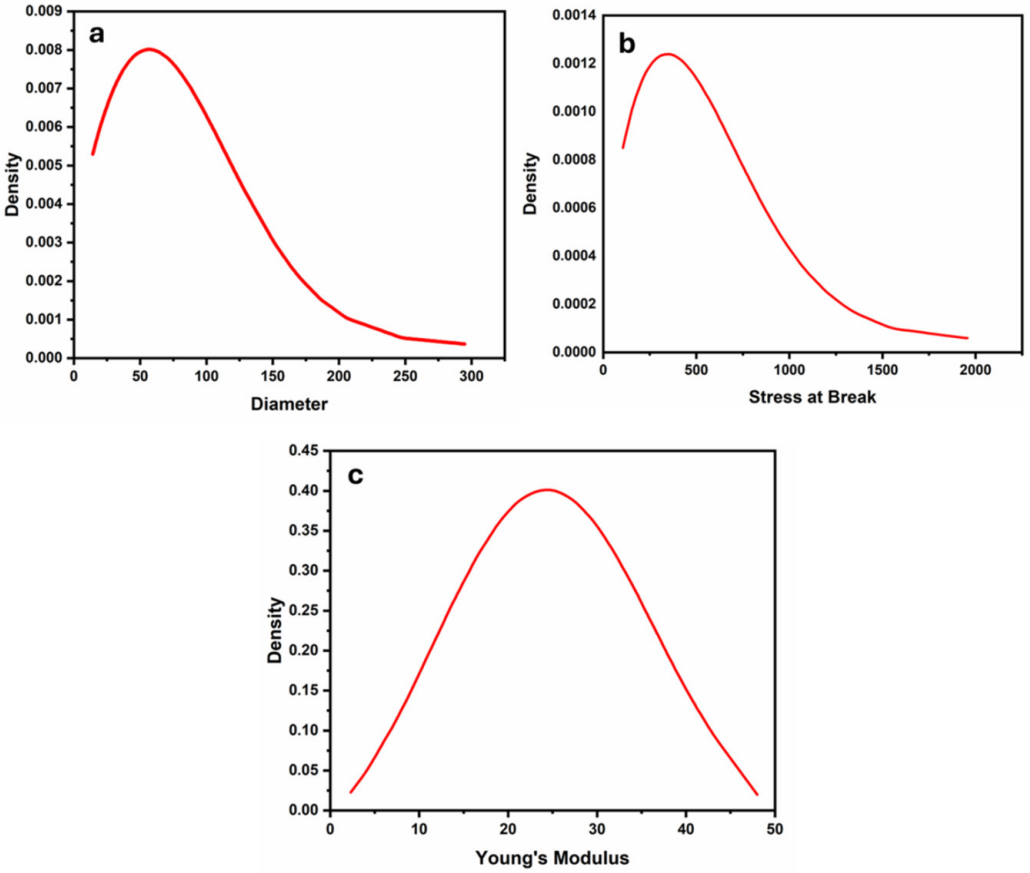

Figure 6. Probability Density Function (PDF) from Equation (3) for (**a**) diameter, (**b**) stress at break, and (**c**) Young's modulus.

The Probability Density Function (PDF) plots for diameter, stress at break, and Young's modulus, shown in Figure 6, offer critical insights into the distribution and variability of these hemp fiber properties. The asymmetrical shape of these PDF curves highlights the inherent variability within the fibers, with peaks indicating the most probable values for each property. For diameter, the PDF reveals a narrow distribution around a central value, suggesting consistency in fiber thickness. In contrast, the broader PDFs for stress at break and Young's modulus indicate greater variability, reflecting the natural differences in fiber strength and stiffness due to microstructural variations and environmental factors. These distributions are essential for understanding the typical performance characteristics and quality control of hemp fibers, ensuring they meet specific application requirements.

The survival probability plots presented in Figure 7 provide a detailed analysis of the tensile properties of hemp fibers using the 2-parameter Weibull (2P-Weibull) method, offering crucial insights into the reliability and performance of these materials. In Figure 7, the red dots represent the individual data points obtained from experimental measurements of hemp fibers, and blue lines are fitted with survival probability curves, which model the relationship between the measured properties (diameter, stress at break, or Young's modulus) and the survival probability of the fibers. These plots illustrate the likelihood that

the fibers will withstand specific stress levels, stiffness, and strain percentages. The 50% survival probability, a key indicator, represents the median values for tensile strength, Young's modulus, and strain at break, pinpointing the point at which half of the fibers are expected to survive under given conditions. For hemp fibers, the 50% survival probability reveals median values of 97.33 MPa for tensile strength, 3.77 GPa for Young's modulus, and 0.074 for strain. These values align closely with the experimental mean values, demonstrating the consistency and reliability of the fibers' mechanical properties. The survival probability plots thus not only validate the experimental results but also enhance our understanding of the fibers' performance under stress, aiding in the assessment and prediction of their behavior in practical applications. This robust analysis underscores the fibers' suitability for use in various industrial contexts where durability and performance predictability are paramount.

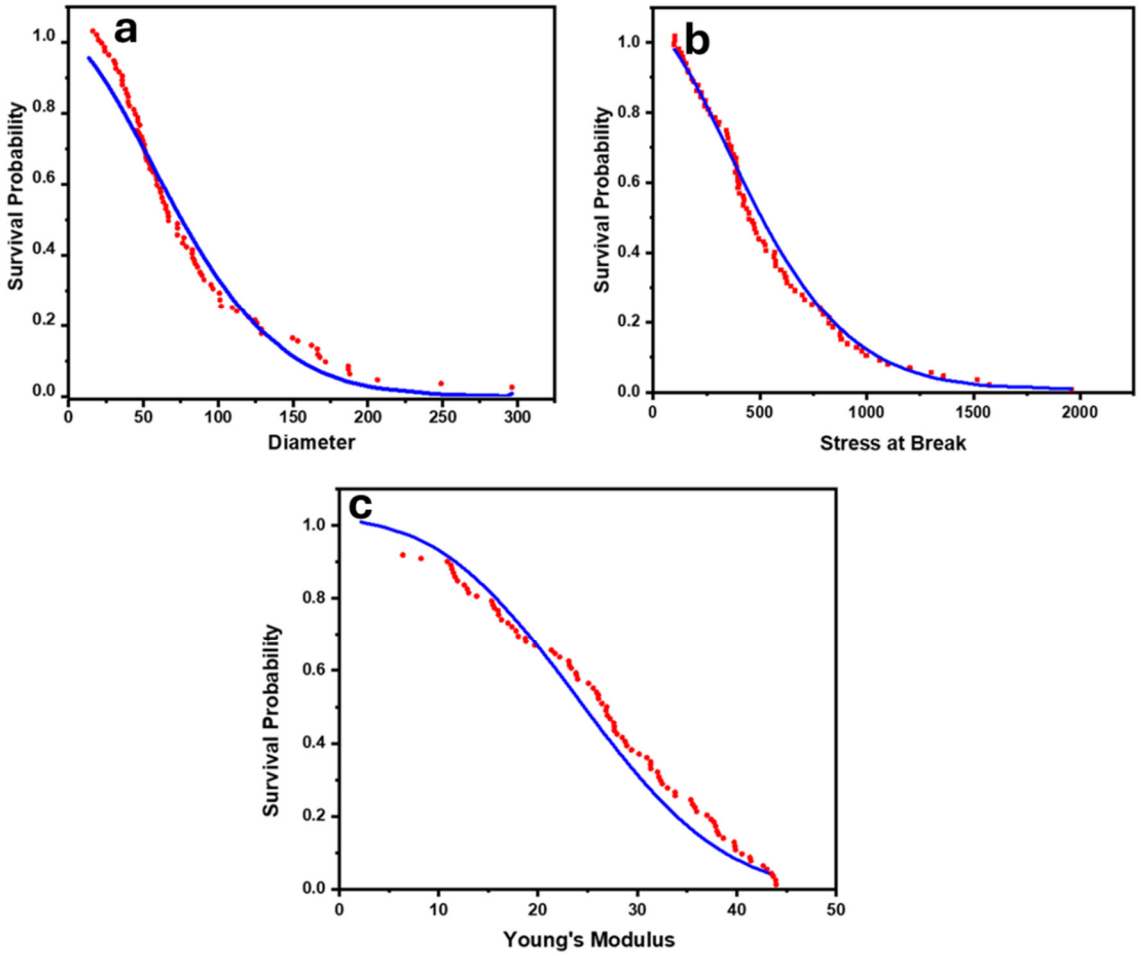

Figure 7. Survival probability plots using 2P-Weibull method for (**a**) diameter, (**b**) stress at break, and (**c**) Young's modulus of hemp fibers. The red dots represent the individual data points obtained from experimental measurements of hemp fibers and blue lines are fitted with survival probability curves.

4.5. Griffith Distribution Analysis

The Griffith analysis provides an understanding of the relationship between fiber diameter and tensile properties, specifically focusing on tensile strength and Young's modulus. By modeling these relationships, the analysis yields parameters A and B that quantitatively describe how these properties change with varying diameters. Figure 8 represents the Griffith analysis of the hemp fiber properties. This trend is characteristic of natural fibers, where larger diameters often correlate with greater structural flaws and inconsistencies, leading to reduced strength. Similarly, for Young's modulus, parameters A = 26.43 GPa and B = −0.13 MPa·μm suggest a slight inverse relationship with diameter.

This finding is consistent with other natural fibers, where thicker fibers typically exhibit lower structural integrity, resulting in a decrease in stiffness. These insights from the Griffith analysis not only align with observed behaviors in natural fibers but also provide critical data for predicting and optimizing the performance of hemp fibers in various applications. Understanding these diameter-dependent variations in tensile properties is essential for material selection and engineering processes, ensuring that fibers meet specific performance criteria in industrial and composite material applications.

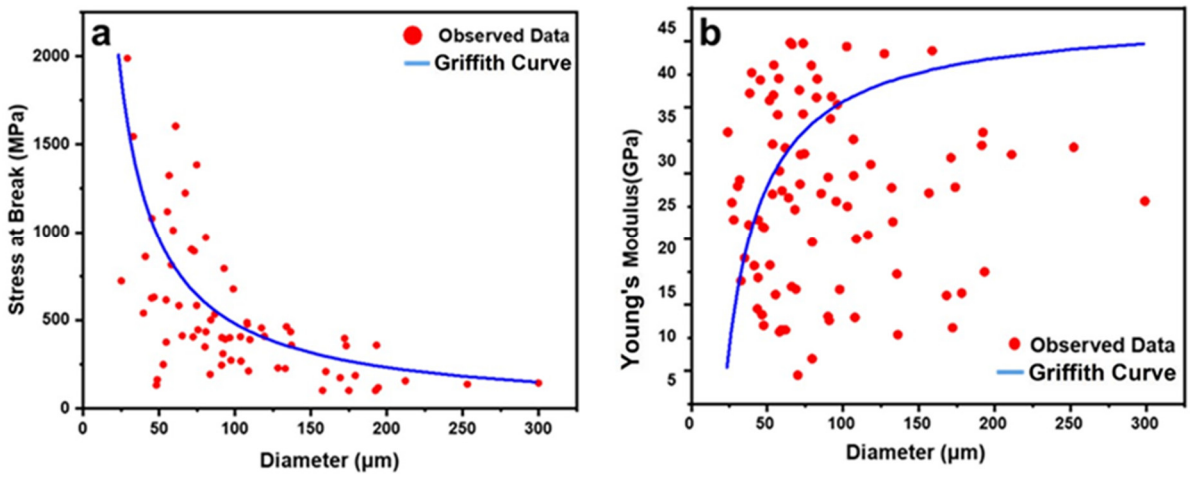

Figure 8. Application of Griffith model to hemp fiber bundles for: (**a**) stress at break as a function of fiber diameter, and (**b**) Young's modulus as a function of fiber diameter. The red points represent observed experimental data, while the blue curve shows the theoretical predictions based on the Griffith model.

5. Conclusions

The results obtained from the tensile test conducted on more than two hundred samples of hemp fibers revealed substantial variability in the tensile strength results between samples. This is consistent with existing literature showing that hemp fibers exhibit a wide range of strengths from sample to sample. The high degree of variation implies that the sampling method and geometry significantly influenced the test outcomes. Closer examination of the data indicates a pattern, as the diameter of the tested fiber segments decreased, their specific strength (strength per unit area) increased. This suggests that defects and weak points concentrated in the larger diameter samples, lowering their overall strength. Another factor may be that multiple fibers are bundled in the larger segments versus pristine single fibers are more likely in the narrower segments.

Moreover, the considerable spread in strengths underscores the sensitivity of natural hemp fibers to sampling effects. Proper isolation and testing of defect-free single fiber specimens is needed to determine the true inherent tensile strength. Statistical analysis of the current dataset could help estimate single fiber strength by focusing on the highest strength values, which are less affected by defects. Tighter control over sampling and geometry should improve consistency, but some variability is expected with natural materials like hemp, necessitating robust testing of many samples. It is worth noting that the power regression model assumes a continuous and smooth relationship between tensile strength and stiffness, as well as fiber bundle diameter. There may be additional complexities or discontinuities in the relationships, particularly at smaller or larger diameter ranges, which could potentially be better captured by alternative models or piecewise functions.

Author Contributions: Conceptualization, Q.W. and Q.C.; methodology, P.S., M.K. and M.S.; writing—original draft preparation, P.S. and R.A.; writing—review and editing Q.C., R.A. and Q.W.; supervision, Q.W.; project administration, Q.W.; funding acquisition, Q.W. All authors have read and agreed to the published version of the manuscript.

Funding: This research was funded by LSU LIFT Fund Grant Program [AG-2023-LIFT-001] and the Louisiana Board of Regents [LEQSF(2020-23)-RD-B-02].

Data Availability Statement: Data will be provided upon request.

Acknowledgments: The authors acknowledge the financial support from the LSU LIFT Fund Grant Program [AG-2023-LIFT-001] and the Louisiana Board of Regents [LEQSF(2020-23)-RD-B-02].

Conflicts of Interest: The authors declare no conflict of interest.

References

1. Kuan, H.T.N.; Tan, M.Y.; Shen, Y.; Yahya, M.Y. Mechanical properties of particulate organic natural filler-reinforced polymer composite: A review. *Compos. Adv. Mater.* **2021**, *30*, 263498332110075. [CrossRef]
2. Sadeghi, B.; Sadeghi, P.; Marfavi, Y.; Kowsari, E.; Zareiyazd, A.A.; Ramakrishna, S. Impacts of cellulose nanofibers on the morphological behavior and dynamic mechanical thermal properties of extruded polylactic acid/cellulose nanofibril nanocomposite foam. *J. Appl. Polym. Sci.* **2022**, *139*, 51673. [CrossRef]
3. Vandepitte, K.; Vasile, S.; Vermeire, S.; Vanderhoeven, M.; Van Der Borght, W.; Latré, J.; De Raeve, A.; Troch, V. Hemp (*Cannabis sativa* L.) for high-value textile applications: The effective long fiber yield and quality of different hemp varieties, processed using industrial flax equipment. *Ind. Crops Prod.* **2020**, *158*, 112969. [CrossRef]
4. Sgriccia, N.; Hawley, M.C.; Misra, M. Characterization of natural fiber surfaces and natural fiber composites. *Compos. Part A Appl. Sci. Manuf.* **2008**, *39*, 1632–1637. [CrossRef]
5. Li, Q.; Hu, C.; Li, M.; Truong, P.; Naik, M.T.; Prabhu, D.; Hoffmann, L.; Rooney, W.L.; Yuan, J.S. Discovering Biomass Structural Determinants Defining the Properties of Plant-Derived Renewable Carbon Fiber. *iScience* **2020**, *23*, 101405. [CrossRef]
6. Sadeghi, P.; Sadeghi, B.; Marfavi, Y.; Kowsari, E.; Ramakrishna, S.; Chinnappan, A. Addressing the Challenge of Microfiber Plastics as the Marine Pollution Crisis Using Circular Economy Methods: A Review. *Mater. Circ. Econ.* **2021**, *3*, 27. [CrossRef]
7. Kumar, S.; Gangil, B.; Mer, K.K.S.; Gupta, M.K.; Patel, V.K. Bast Fiber-Based Polymer Composites. In *Hybrid Fiber Composites*, 1st ed.; Khan, A., Rangappa, S.M., Jawaid, M., Siengchin, S., Asiri, A.M., Eds.; Wiley: New York, NY, USA, 2020; pp. 147–167. [CrossRef]
8. Alsubari, S.; Zuhri, M.Y.M.; Sapuan, S.M.; Ishak, M.R.; Ilyas, R.A.; Asyraf, M.R.M. Potential of Natural Fiber Reinforced Polymer Composites in Sandwich Structures: A Review on Its Mechanical Properties. *Polymers* **2021**, *13*, 423. [CrossRef]
9. Karimah, A.; Ridho, M.R.; Munawar, S.S.; Adi, D.S.; Ismadi Damayanti, R.; Subiyanto, B.; Fatriasari, W.; Fudholi, A. A review on natural fibers for development of eco-friendly bio-composite: Characteristics, and utilizations. *J. Mater. Res. Technol.* **2021**, *13*, 2442–2458. [CrossRef]
10. Liu, M.; Fernando, D.; Daniel, G.; Madsen, B.; Meyer, A.S.; Ale, M.T.; Thygesen, A. Effect of harvest time and field retting duration on the chemical composition, morphology and mechanical properties of hemp fibers. *Ind. Crops Prod.* **2015**, *69*, 29–39. [CrossRef]
11. Promhuad, K.; Srisa, A.; San, H.; Laorenza, Y.; Wongphan, P.; Sodsai, J.; Tansin, K.; Phromphen, P.; Chartvivatpornchai, N.; Ngoenchai, P.; et al. Applications of Hemp Polymers and Extracts in Food, Textile and Packaging: A Review. *Polymers* **2022**, *14*, 4274. [CrossRef]
12. Shoul, B.; Marfavi, Y.; Sadeghi, B.; Kowsari, E.; Sadeghi, P.; Ramakrishna, S. Investigating the potential of sustainable use of green silica in the green tire industry: A review. *Environ. Sci. Pollut. Res.* **2022**, *29*, 51298–51317. [CrossRef] [PubMed]
13. Tanasă, F.; Zănoagă, M.; Teacă, C.; Nechifor, M.; Shahzad, A. Modified hemp fibers intended for fiber-reinforced polymer composites used in structural applications—A review. I. Methods of modification. *Polym. Compos.* **2020**, *41*, 5–31. [CrossRef]
14. Thygesen, A.; Daniel, G.; Lilholt, H.; Thomsen, A.B. Hemp Fiber Microstructure and Use of Fungal Defibration to Obtain Fibers for Composite Materials. *J. Nat. Fibers* **2006**, *2*, 19–37. [CrossRef]
15. Placet, V.; Méteau, J.; Froehly, L.; Salut, R.; Boubakar, M.L. Investigation of the internal structure of hemp fibres using optical coherence tomography and Focused Ion Beam transverse cutting. *J. Mater. Sci.* **2014**, *49*, 8317–8327. [CrossRef]
16. Kalia, S.; Kaith, B.S. Use of Flax-g-poly (MMA) as Reinforcing Material for Enhancement of Properties of Phenol Formaldehyde Composites. *Int. J. Polym. Anal. Charact.* **2008**, *13*, 341–352. [CrossRef]
17. Le Troedec, M.; Sedan, D.; Peyratout, C.; Bonnet, J.P.; Smith, A.; Guinebretiere, R.; Gloaguen, V.; Krausz, P. Influence of various chemical treatments on the composition and structure of hemp fibres. *Compos. Part A Appl. Sci. Manuf.* **2008**, *39*, 514–522. [CrossRef]
18. Manaia, J.P.; Manaia, A.T.; Rodriges, L. Industrial Hemp Fibers: An Overview. *Fibers* **2019**, *7*, 106. [CrossRef]
19. Bleuze, L.; Chabbert, B.; Lashermes, G.; Recous, S. Hemp harvest time impacts on the dynamics of microbial colonization and hemp stems degradation during dew retting. *Ind. Crops Prod.* **2020**, *145*, 112122. [CrossRef]
20. Basu, B.; Tiwari, D.; Kundu, D.; Prasad, R. Is Weibull distribution the most appropriate statistical strength distribution for brittle materials? *Ceram. Int.* **2009**, *35*, 237–246. [CrossRef]
21. Li, T.; Griffiths, W.D.; Chen, J. Weibull Modulus Estimated by the Non-linear Least Squares Method: A Solution to Deviation Occurring in Traditional Weibull Estimation. *Metall. Mater. Trans. A* **2017**, *48*, 5516–5528. [CrossRef]
22. Benjeddou, O. Weibull statistical analysis and experimental investigation of size effects on tensile behavior of dry unidirectional carbon fiber sheets. *Polym. Test.* **2020**, *86*, 106498. [CrossRef]

23. Devi, L.U.; Bhagawan, S.S.; Thomas, S. Mechanical properties of pineapple leaf fiber-reinforced polyester composites. *J. Appl. Polym. Sci.* **1997**, *64*, 1739–1748. [CrossRef]
24. Wallenberger, F.T. Introduction to Reinforcing Fibers. In *Composites*; Miracle, D.B., Donaldson, S.L., Eds.; ASM International: Almere, The Netherlands, 2001; pp. 23–26. [CrossRef]
25. Chokshi, S.; Parmar, V.; Gohil, P.; Chaudhary, V. Chemical Composition and Mechanical Properties of Natural Fibers. *J. Nat. Fibers* **2022**, *19*, 3942–3953. [CrossRef]
26. Lu, C.; Wang, C.H.; Li, C.H.; Tong, J.F.; Sun, Y.F. Structural and Mechanical Properties of Hemp Fibers: Effect of Progressive Removal of Hemicellulose and Lignin. *J. Nat. Fibers* **2022**, *19*, 13985–13994. [CrossRef]
27. Lu, N.; Oza, S. A comparative study of the mechanical properties of hemp fiber with virgin and recycled high density polyethylene matrix. *Compos. Part B Eng.* **2013**, *45*, 1651–1656. [CrossRef]
28. Masirek, R.; Kulinski, Z.; Chionna, D.; Piorkowska, E.; Pracella, M. Composites of poly(L-lactide) with hemp fibers: Morphology and thermal and mechanical properties. *J. Appl. Polym. Sci.* **2007**, *105*, 255–268. [CrossRef]
29. Niu, P.; Liu, B.; Wei, X.; Wang, X.; Yang, J. Study on mechanical properties and thermal stability of polypropylene/hemp fiber composites. *J. Reinf. Plast. Compos.* **2011**, *30*, 36–44. [CrossRef]
30. Ribeiro, J.; Bueno, G.; Martín, M.R.; Rocha, J. Experimental Study on Mechanical Properties of Hemp Fibers Influenced by Various Parameters. *Sustainability* **2023**, *15*, 9610. [CrossRef]
31. Oseli, A.; Bizjan, B.; Król, E.; Širok, B.; Slemenik Perše, L. Tensile properties of mineral fibers determined with Sentmanat extensional rheometer. *Constr. Build. Mater.* **2020**, *253*, 119215. [CrossRef]
32. Lu, D.; Yu, W.; Pan, N. Determination of the strength and elongation distribution of single wool through fiber bundle testing based on acoustic emissions. *Text. Res. J.* **2021**, *91*, 1263–1273. [CrossRef]
33. Eichhorn, S.J.; Young, R.J. Composite micromechanics of hemp fibres and epoxy resin microdroplets. *Compos. Sci. Technol.* **2004**, *64*, 767–772. [CrossRef]
34. Shivnand, H.K.; Inamdar, P.S.; Sapthagiri, G. Evaluation of tensile and flexural properties of hemp and polypropylene based natural fiber composites. In Proceedings of the 2010 2nd International Conference on Chemical, Biological and Environmental Engineering, Cairo, Egypt, 2–4 November 2010; pp. 90–95. [CrossRef]
35. Takemura, K.; Minekage, Y. Effect of molding condition on tensile properties of hemp fiber reinforced composite. *Adv. Compos. Mater.* **2007**, *16*, 385–394. [CrossRef]
36. *ASTM D3379-75*; Standard Test Method for Tensile Strength and Young's Modulus for High Modulus Single Filament Fibers. ASTM Standards: West Conshohocken, PA, USA, 1975.
37. Jawaid, M.; Abdul Khalil, H.P.S. Cellulosic/Synthetic fibre reinforced polymer hybrid composites: A review. *Carbohydr. Polym.* **2011**, *86*, 1–18. [CrossRef]
38. Wang, Y.; Yu, W.; Wang, F. Experimental evaluation and modified Weibull characterization of the tensile behavior of tri-component elastic-conductive composite yarn. *Text. Res. J.* **2018**, *88*, 1138–1149. [CrossRef]
39. Hallinan, A.J. A Review of the Weibull Distribution. *J. Qual. Technol.* **1993**, *25*, 85–93. [CrossRef]
40. Duval, A.; Bourmaud, A.; Augier, L.; Baley, C. Influence of the sampling area of the stem on the mechanical properties of hemp fibers. *Mater. Lett.* **2011**, *65*, 797–800. [CrossRef]
41. Griffith, A.A., VI. The phenomena of rupture and flow in solids. *Philos. Trans. R. Soc. Lond. Ser. A Contain. Pap. A Math. Phys. Character* **1921**, *221*, 163–198. [CrossRef]
42. Cattin, P. Estimation of the predictive power of a regression model. *J. Appl. Psychol.* **1980**, *65*, 407–414. [CrossRef]
43. Chai, T.; Draxler, R.R. Root mean square error (RMSE) or mean absolute error (MAE)? *Geosci. Model Dev.* **2014**, *7*, 1247–1250. [CrossRef]